

## Supplementary Information

### **Practical production of heteroatom-bridged and mixed amorphous-crystalline silicon for stable and fast-charging batteries**

Minjun Je,<sup>‡a</sup> Gyujin Song,<sup>‡ad</sup> Sangyeop Lee,<sup>b</sup> Hyun Jung Park,<sup>c</sup> Joohyuk Kim,<sup>c</sup> Soojin Park<sup>\*ab</sup>

<sup>a</sup>Department of Chemistry, Pohang University of Science and Technology (POSTECH), Pohang 37673, Republic of Korea.

<sup>b</sup>Division of Advanced Materials Science, Pohang University of Science and Technology (POSTECH), Pohang 37673, Republic of Korea

<sup>c</sup>LK Technology, Gyeongju 38214, Republic of Korea

<sup>d</sup>Ulsan Advanced Energy Technology R&D Center, Korea Institute of Energy Research (KIER), Ulsan 44776, Republic of Korea

<sup>‡</sup> These authors equally contributed this work

\*Corresponding author: soojin.park@postech.ac.kr

## Table of Contents

- Table S1.** The comparison table of recently reported Si-based anodes.
- Fig. S1** Photograph images of liter-scale reactor and production yield.
- Fig. S2** Step-by-step XRD patterns on synthetic process.
- Fig. S3** Morphological characterization of Control sample.
- Fig. S4** SEM image of MACS.
- Fig. S5** Comparison of tap densities.
- Fig. S6** FT-IR spectra of Control and MACS.
- Fig. S7** Calculated data of crystallite size.
- Fig. S8** TOF-SIMS depth profiling results.
- Fig. S9** Galvanostatic charge/discharge profiles at formation cycle in half-cell.
- Fig. S10** Electrochemical properties of high mass-loaded MACS anode.
- Fig. S11** XPS spectra of MACS electrode after 50 cycles in O 1s.
- Fig. S12** Dark-field TEM image of MACS structure after 50 cycles and corresponding elemental mapping.
- Fig. S13** Nyquist plots for cycled electrodes.
- Fig. S14** Cross-sectional SEM images for cycled electrodes.
- Fig. S15** Rate capability at various C-rates.
- Fig. S16** Morphological/Electrochemical characterization of NCM622 cathode.
- Fig. S17** Galvanostatic charge/discharge profiles at formation cycle in full cell.

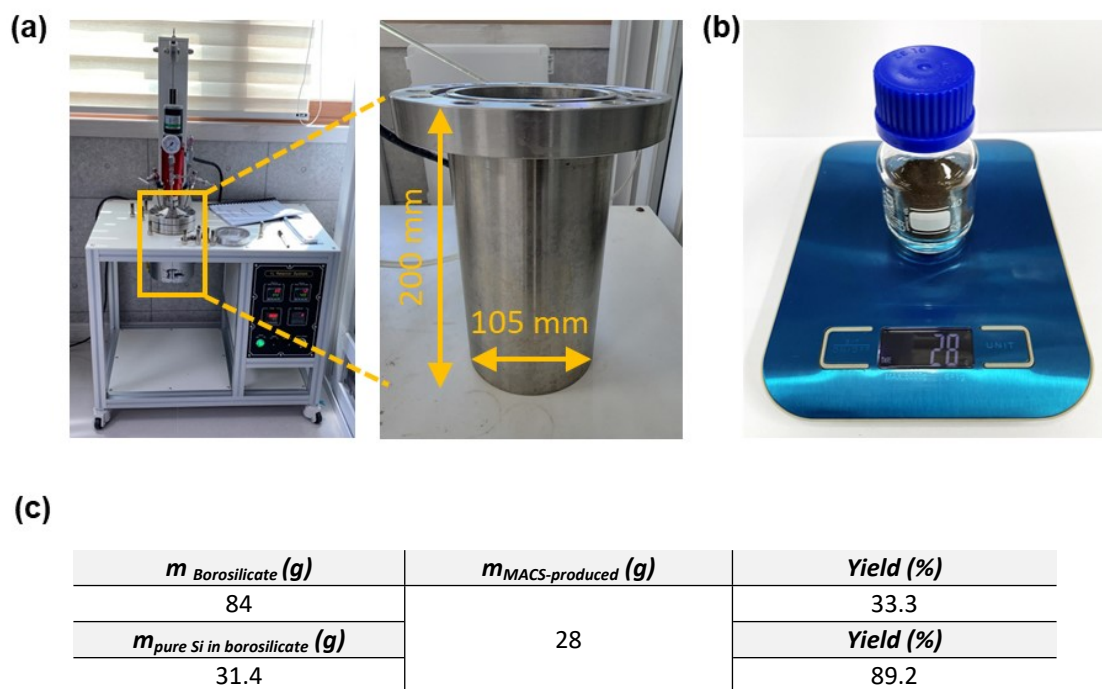


**Fig. S1** (a) Custom-made liter-scale reactor system setup and reactor size. (b) The production yield of MACS in a single batch. (c) Production yield of practical MACS synthesis.

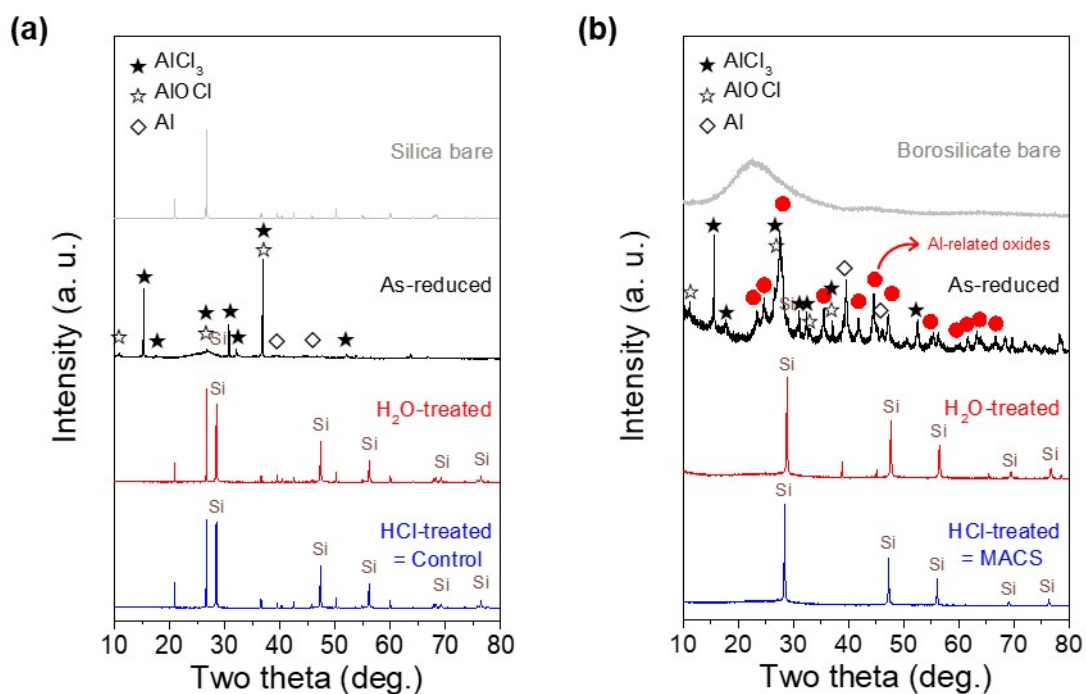


**Fig. S2** Step-by-step XRD patterns of (a) Control and (b) MACS.

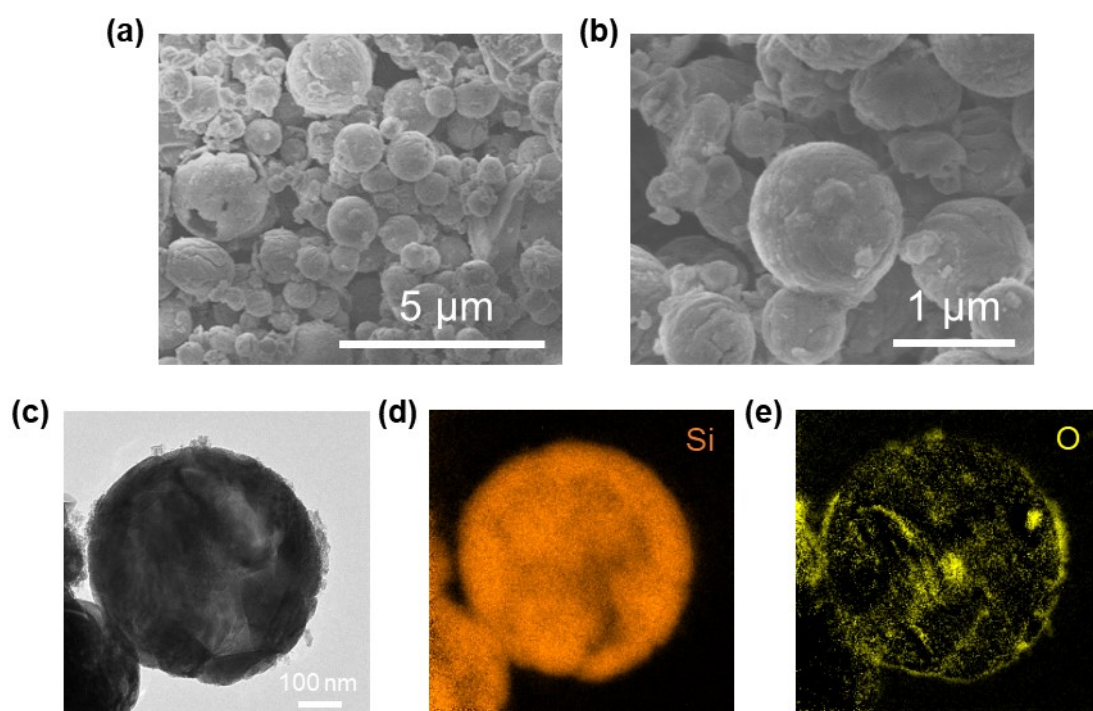


**Fig. S3** (a, b) SEM images, (c) TEM image and (d, e) elemental mapping of Control sample.

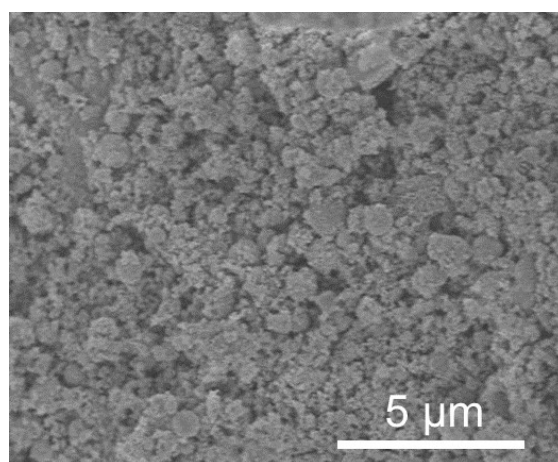
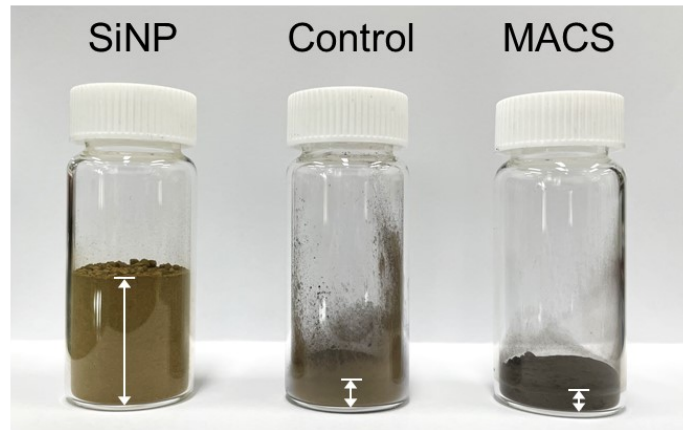


**Fig. S4** Low magnified SEM image of MACS.



	SiNP	Control	MACS
Tap density (g m <sup>-3</sup> )	0.091	0.413	0.531

Fig. S5 Tap densities of commercial Si nanoparticle (~50 nm), Control, and MACS powders.

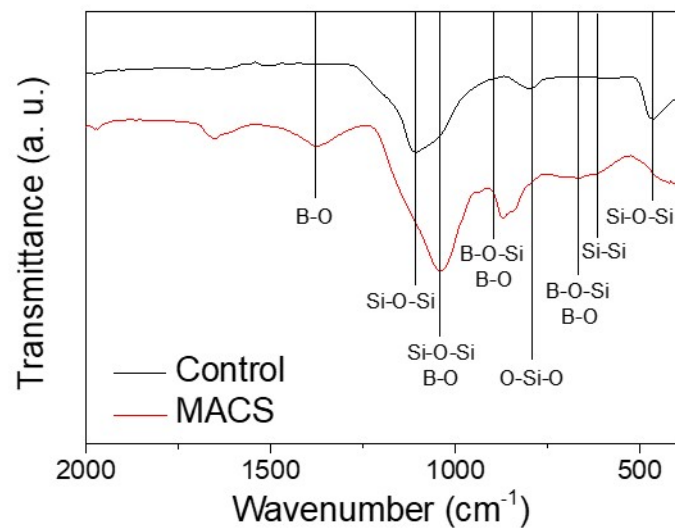
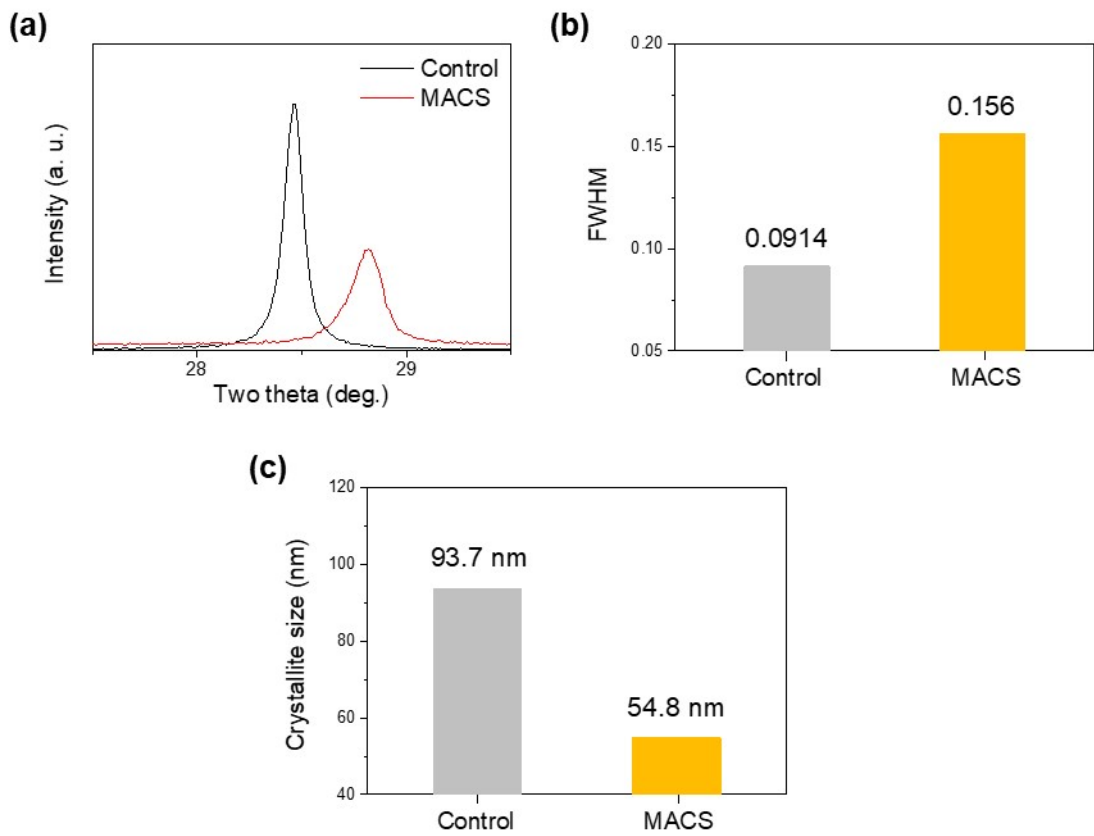
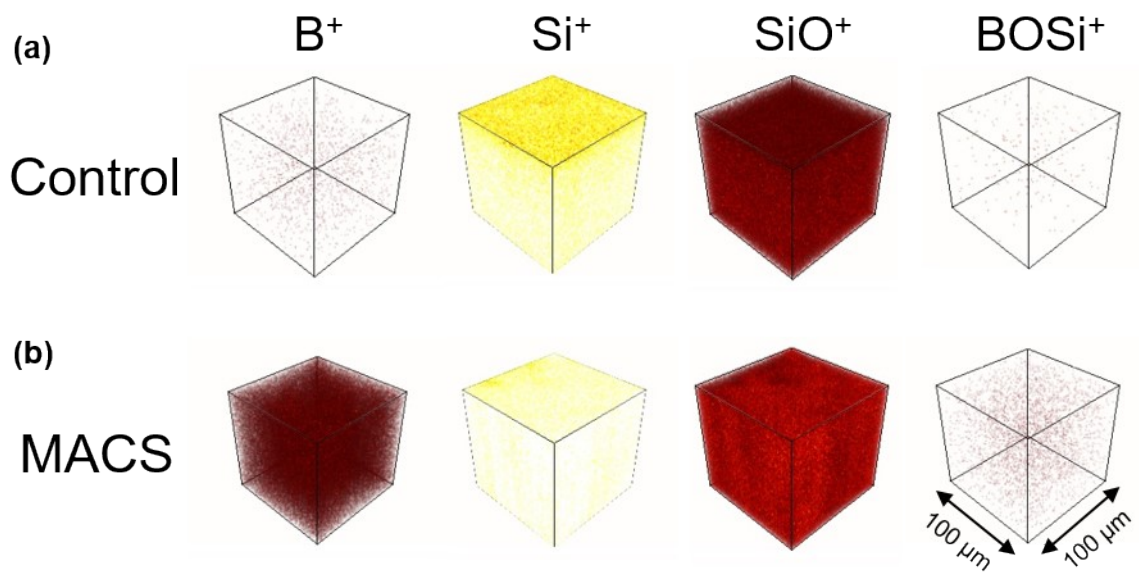


Fig. S6 FT-IR spectra of (a) Control and (b) MACS particles.



**Fig. S7** (a) XRD patterns of Control and MACS in the two-theta range of 27.5-29.5°. (b) Calculated FWHM values and (c) the corresponding crystallite size of Control and MACS.



**Fig. S8** TOF-SIMS depth profiling results. Three-dimensional mapping of (a) Control and (b) MACS.

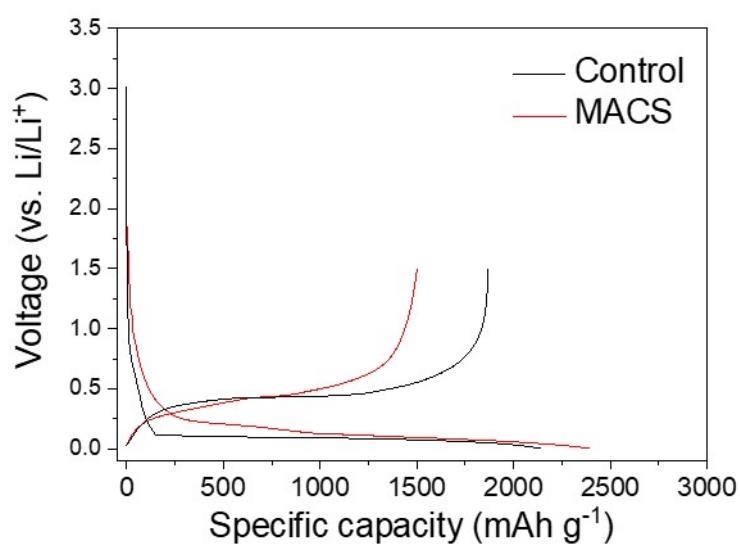


**Fig. S9** Galvanostatic charge/discharge profiles of Control and MACS electrodes at 0.05 C.

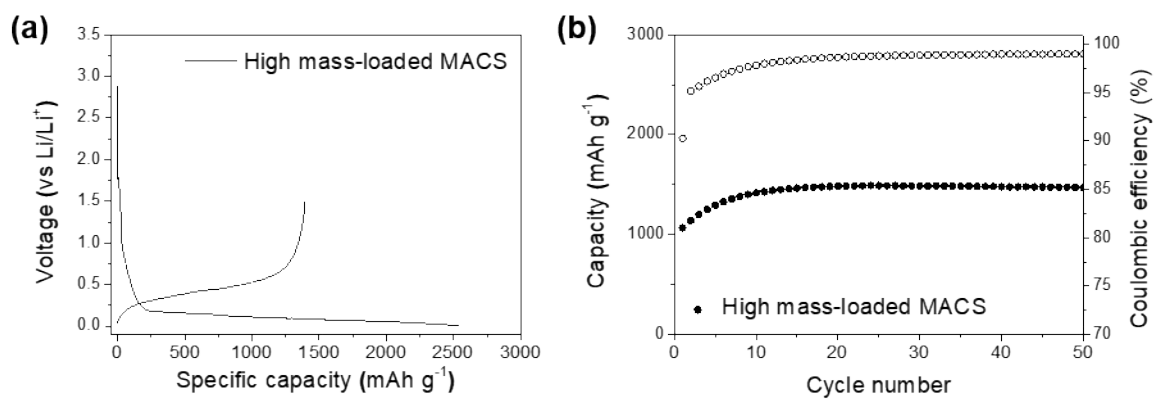


**Fig. S10** Electrochemical properties of high mass-loaded MACS anode. (1.4 mg cm<sup>-2</sup>). (a) Galvanostatic charge/discharge profile at the formation cycle. (b) Cycle retention at 0.2 C



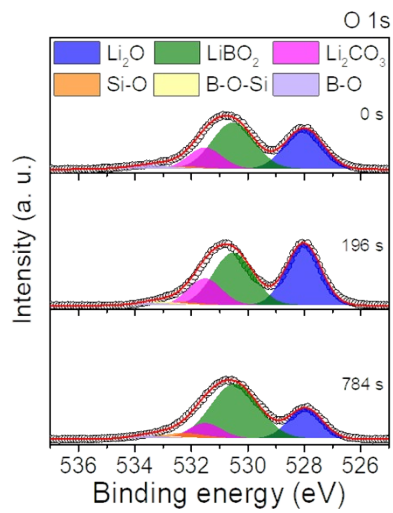


**Fig. S11** XPS spectra of MACS electrode after 50 cycles in O 1s.

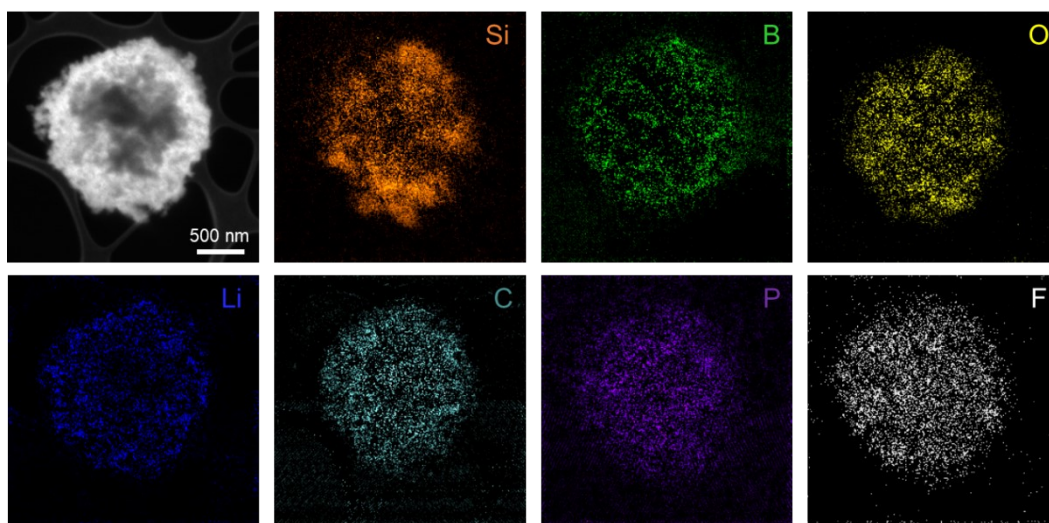


**Fig. S12** Dark-field TEM image of MACS structure after 50 cycles and corresponding elemental mapping.



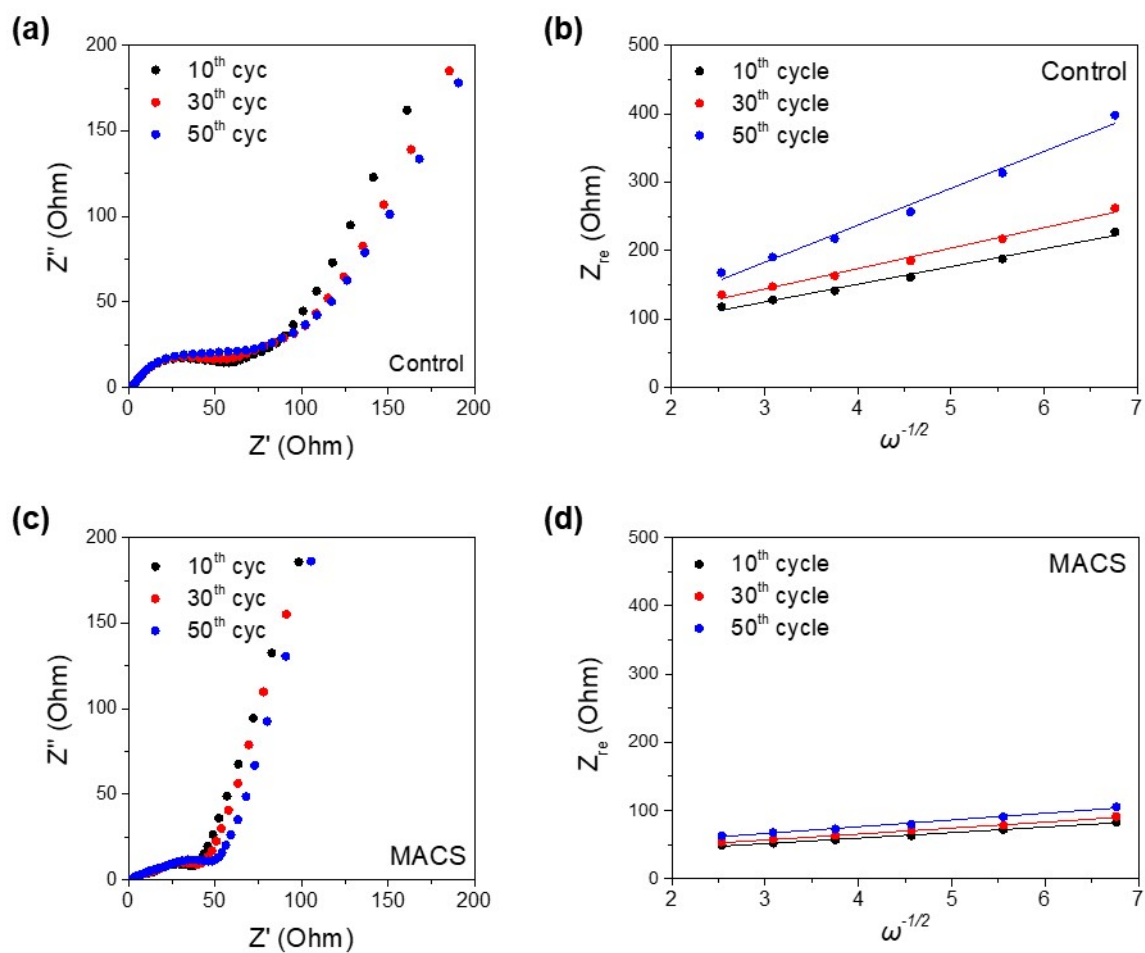


**Fig. S13** Nyquist plots of (a) Control and (c) MACS electrodes after 10, 30, 50 cycles at 0.5 C, and the corresponding linear fitting of Warburg impedance of (b) Control and (d) MACS electrodes.

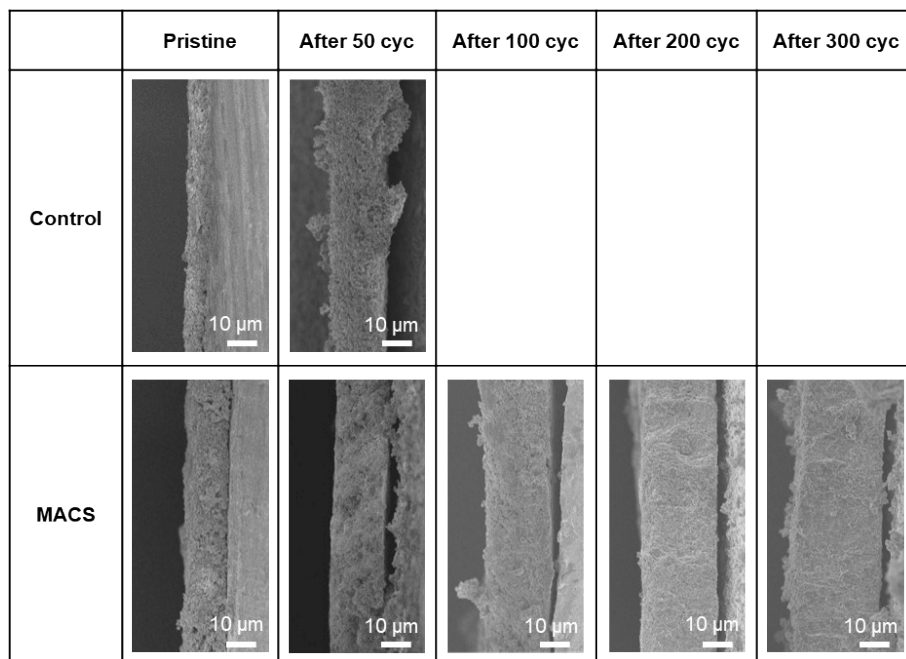


**Fig. S14** Cross-sectional SEM images of Control and MACS electrodes: pristine and after 50, 100, 200 and 300 cycles.

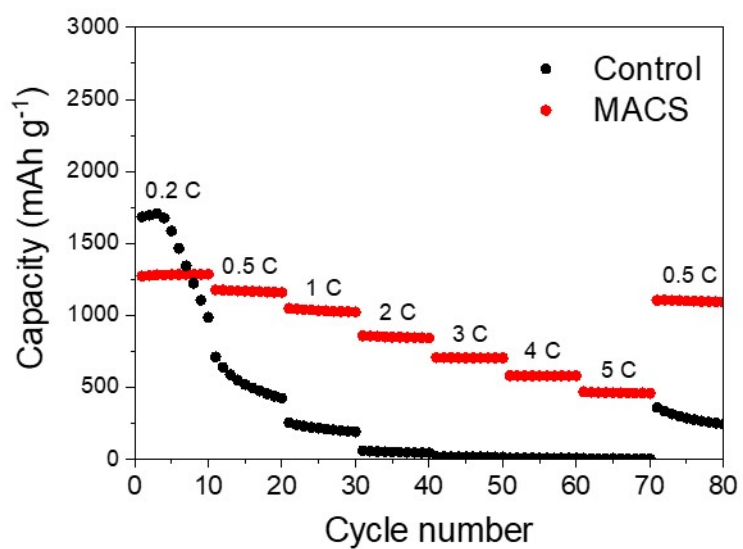


**Fig. S15** Rate capability of Control and MACS anodes at various C-rates.

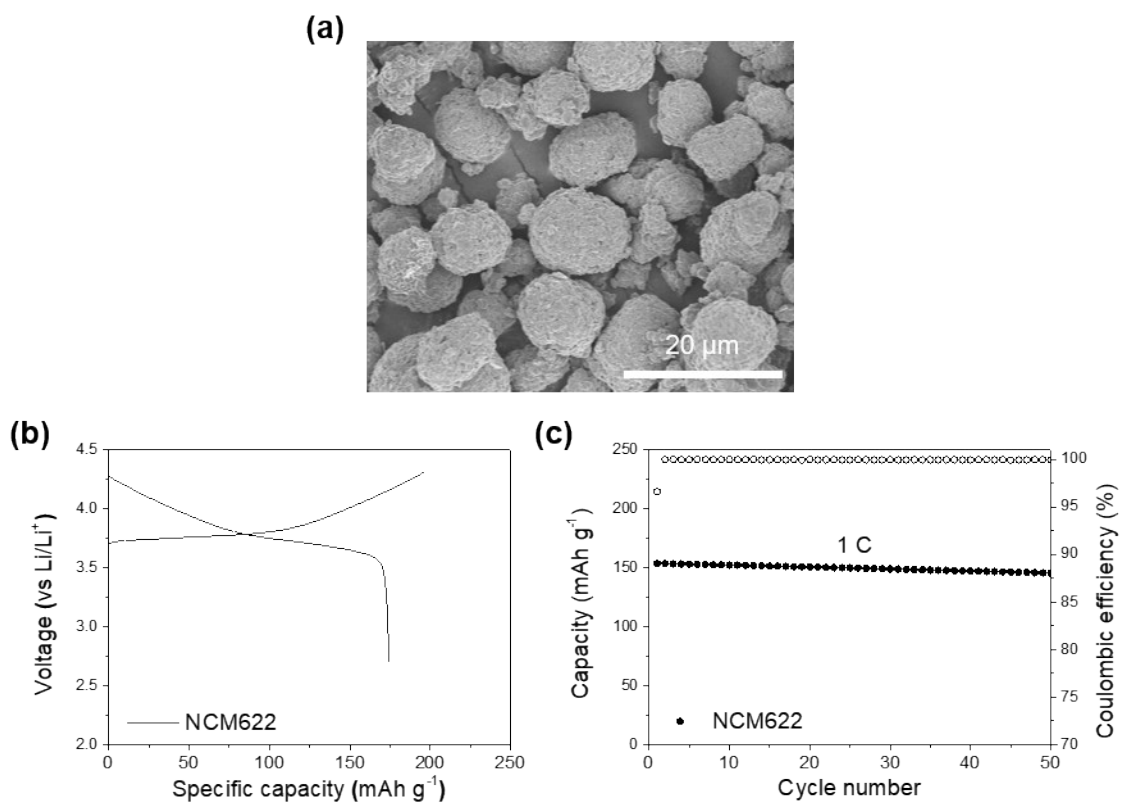


**Fig. S16** (a) SEM image of NCM622. (a) Galvanostatic charge/discharge profiles of NCM622 electrode at 0.1 C. (b) Cycling stability of NCM 622 electrode at 1 C.

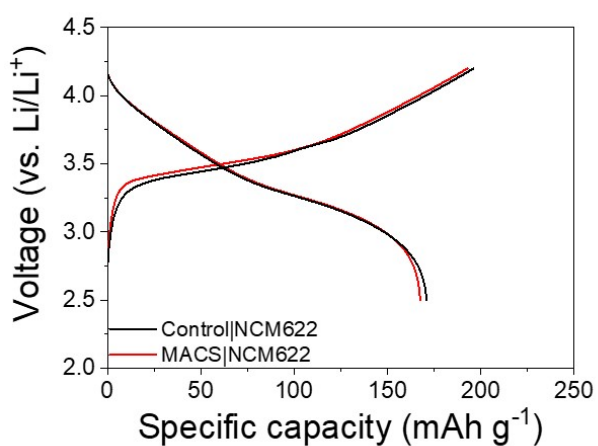


**Fig. S17** Galvanostatic charge/discharge profiles of full cell using pre-lithiated Control and MACS anodes and NCM622 cathode at 0.1 C.

**Table S1.** The comparison table of recently reported Si-based anodes.

Sample	Current density (A g <sup>-1</sup> )	Cycle life (n)	Capacity retention: X%@Y cycle	Reference
Si@GG-g-PAM	1	200	60.5%@200 cycle	1
Si+rGO@DFAT-C	0.5	200	63%@200 cycle	2
SC-G	1	300	65%@300 cycle	3
Si-NH <sub>2</sub> @PAA-DA	0.4	100	68.8%@100 cycle	4
Si-Sn@C400-2	1.5	500	51.7%@500 cycle	5
Si@CTSC	1	200	76.1%@200 cycle	6
Si/PAA-TUEG	2.1	300	82%@300 cycle	7
<b>MACS</b>	<b>1.5</b>	<b>500</b> <b>1000</b>	<b>90.8%@500 cycle</b> <b>70.4%@1000 cycle</b>	<b><i>This work</i></b>

## References

- 1 Z. Li, G. Wu, Y. Yang, Z. Wan, X. Zeng, L. Yan, S. Wu, M. Ling, C. Liang, K. N. Hui, Z. Lin, *Adv. Energy Mater.*, 2022, **12**, 2201197.
- 2 Q. Wang, T. Meng, Y. Li, J. Yang, B. Huang, S. Ou, C. Meng, S. Zhang, Y. Tong, *Energy Storage Mater.*, 2021, **39**, 354-364.
- 3 R. F. H. Hernandha, P. C. Rath, B. Umesh, J. Patra, C.-Y. Huang, W.-W. Wu, Q.-F. Dong, J. Li, J.-K. Chang, *Adv. Funct. Mater.*, 2021, **31**, 2104135.
- 4 X. Wan, T. Mu, B. Shen, Q. Meng, G. Lu, S. Lou, P. Zuo, Y. Ma, C. Du, G. Yin, *Nano Energy*, 2022, **99**, 107334.
- 5 Z. Dong, W. Du, C. Yan, C. Zhang, G. Chen, J. Chen, W. Sun, Y. Jiang, Y. Liu, M. Gao, J. Gan, Y. Yang, H. Pan, *ACS Appl. Mater. Interfaces*, 2021, **13**, 45578-45588.
- 6 R. Shao, F. Zhu, Z. Cao, Z. Zhang, M. Dou, J. Niu, B. Zhu, F. Wang, *J. Mater. Chem. A*, 2020, **8**, 18338-18347.
- 7 H. Liu, Q. Wu, X. Guan, M. Liu, F. Wang, R. Li, J. Xu, *ACS Appl. Energy Mater.*, 2022, **5**, 4934-4944.